

# PROPERTIES OF SEMICONDUCTING $\text{Ru}_2\text{Ge}_3$

Jean-Pierre Fleurial and Alex Borshchevsky

Jet Propulsion Laboratory/ California Institute of Technology,  
MS 277-212, 4800 Oak Grove Dr., Pasadena, CA 91109, USA

## ABSTRACT

Transport properties of large single crystalline samples of  $\text{Ru}_2\text{Ge}_3$  grown from the melt have been investigated in a 25-1000 C temperature range. A diffusionless transition between 500 and 550 C from a high temperature tetragonal structure to a low temperature orthorhombic structure was clearly observed. Results showed that both the low temperature orthorhombic and the high temperature structural tetragonal phase are semiconductors. Some anisotropy of the transport coefficients was determined by measuring the samples in orientations parallel and perpendicular to the preferential direction of crystal growth. Large Seebeck coefficient (up to  $400 \mu\text{VK}^{-1}$ ) and low thermal conductivity (as low as  $20 \times 10^{-3} \text{Wcm}^{-1}\text{K}^{-1}$ ) were achieved for the low temperature orthorhombic phase. Difficulties in preparing heavily doped samples and low Hall mobilities have limited values for the maximum figure of merit to  $0.5 \times 10^{-3} \text{K}^{-1}$  at 500 C.

## INTRODUCTION

Extensive theoretical and experimental studies have resulted in reasonable improvements in the dimensionless figure of merit  $ZT$  (up to 50%) of the state of the art high temperature thermoelectric  $\text{Si}_{80}\text{Ge}_{20}$  alloys in the last 5 years [1]. However, significantly higher material conversion efficiencies are needed to make thermoelectrics competitive and economically attractive. A new approach [2, 3] that looks at radically different compounds and alloys was recently started at the Jet Propulsion Laboratory (JPL). Several Si-rich transition metal silicides with high melting point, complex crystal structure and high density were identified as high temperature semiconductors with good potential for high  $ZT$  values [4]. In parallel with the study of  $\text{Ru}_2\text{Si}_3$ , preparation and high temperature transport properties of  $\text{Ru}_2\text{Ge}_3$  have been investigated at JPL.

Ruthenium sesquigermanide,  $\text{Ru}_2\text{Ge}_3$ , and its isostructural analogs  $\text{Ru}_2\text{Si}_3$  and  $\text{Ru}_2\text{Sn}_3$ , are known as "chimney-ladder" compounds characterized by long tetragonal unit cells consisting of  $\beta$ -tin type subcells of Ru atoms stacked one on top of the other, and a helical arrangement of the other Ge, Si or Sn atoms [5]. They have been shown to undergo a diffusionless phase transformation from an orthorhombic centro-symmetric low temperature structure to a tetragonal non-centrosymmetric high temperature structure [6]. These transformations, due to short displacements of the Ge, Si or Sn atoms, are reversible and occur gradually over a wide temperature range. Some properties of these compounds were previously investigated by preparing several re-meltings of the elements in RF and arc furnaces until the final products contained only single phase defined by metallography and X-ray powder diffraction analysis [6,7].  $\text{Ru}_2\text{Si}_3$  and  $\text{Ru}_2\text{Ge}_3$  compounds demonstrated semiconducting properties with high temperature modifications energy gaps of 0.44 and 0.34 eV, respectively. These gaps increase discontinuously while the compounds undergo diffusionless phase transformations into the low temperature modifications,  $\text{Ru}_2\text{Ge}_3$  decomposes peritectically at a temperature of 1470°C [8]. Growth of  $\text{Ru}_2\text{Ge}_3$  can be achieved by crystallization of slightly off-stoichiometric Ge-rich solutions.

## EXPERIMENTAL DETAILS

Growth experiments with various Ru and Ge compositions showed that good quality single phase  $\text{Ru}_2\text{Ge}_3$  samples could be obtained from melts containing 38 at. % Ru and 62 at. % Ge [9]. Crystallization from compositions closer to the 2:3 stoichiometric ratio resulted in incisions of RuGe, thus demonstrating that the peritectic plateau of  $\text{Ru}_2\text{Ge}_3$  extended to 62 at. % (it. Polycrystalline ingots, even with grain cross-sections as large as 5-7 mm, were heavily cracked. However, most of the cracks were located at the grain boundaries, thus the crackless single crystalline grains with dimensions of up to 6x6x3 mm<sup>3</sup> were readily available for investigation. Only completely single crystalline ingots were found to be crack-free. Analyses of Laue patterns taken at 25°C from such samples indicated [110] to be the preferential direction of crystal growth [9].

All prepared samples were measured for room temperature Hall effect. Single phase samples of good mechanical strength were also measured for high temperature Hall effect, Seebeck coefficient and thermal conductivity. Because of the complex crystal structure of  $\text{Ru}_2\text{Ge}_3$ , the possible anisotropy of the transport properties had to be taken into account. Most of the thin slices (about 1 mm thick and 10 mm in diameter) were

horizontal cuts and thus Seebeck and thermal conductivity were measured parallel ( $\parallel$ ) to the preferential [110] direction of crystal growth while Hall coefficient and electrical resistivity were measured perpendicular ( $\perp$ ) to the [110] direction of crystal growth.

Some Bridgman grown ingots were mechanically strong enough (few cracks) to allow vertical slices to be cut. On these vertical thin slices, Seebeck coefficient and thermal conductivity were measured  $\perp$  to the [110] direction of crystal growth while Hall coefficient and electrical resistivity were measured  $\parallel$  to the [110] direction of crystal growth. By combining measured properties from both horizontal and vertical cuts located next to each other, anisotropy ratios and values for the figure of merit could be calculated for both the  $\parallel$  and  $\perp$  direction to the [110] direction of crystal growth.

## RESULTS AND DISCUSSION

### Room temperature Hall effect

Measurements, illustrated on Figures 1 and 2, showed that almost all of the investigated samples were of p-type conductivity. Figure 1 shows the decrease in Hall mobility at room temperature with larger carrier concentrations. Highest mobility values obtained for undoped samples were about  $100 \text{ cm}^2 \text{V}^{-1} \text{s}^{-1}$  for a carrier concentration of  $1 \times 10^{17} \text{ cm}^{-3}$ . The highest purity  $\text{Ru}_2\text{Ge}_3$  grown from a 95 at. % Ge solution had the lowest carrier concentration ( $2.4 \times 10^{16} \text{ cm}^{-3}$ ) but the Hall mobility was actually lower ( $50 \text{ cm}^2 \text{V}^{-1} \text{s}^{-1}$ ). Samples doped with a variety of elements show that the mobility decreases little when increasing carrier concentrations from  $10^{17} \text{ cm}^{-3}$  up to  $10^{19} \text{ cm}^{-3}$ , thus effectively lowering the electrical resistivity by almost two orders of magnitude, as seen on Figure 2. However, because mobility values are already low (about 10 to  $40 \text{ cm}^2 \text{V}^{-1} \text{s}^{-1}$ ) the electrical resistivity of these samples still remains one order of magnitude higher than desired (about  $20$  to  $70 \times 10^{-3} \Omega \cdot \text{cm}$  while state of the art thermoelectric materials have electrical resistivity values in the  $0.5$  to  $5 \times 10^{-3} \Omega \cdot \text{cm}$  range).

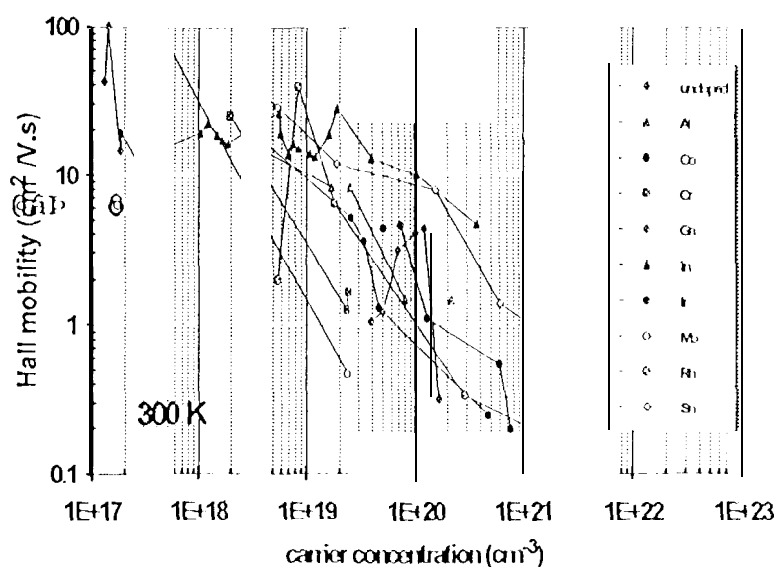


Figure 1 Room temperature Hall mobility versus carrier concentration for doped and undoped  $\text{Ru}_2\text{Ge}_3$  samples.

Higher dopant concentrations using transition metal elements such as Co, Cr, Ir, Mn, h40, Ni, Pt, Re and Rh either did not succeed in increasing carrier concentrations or resulted in an very fast degradation of the mobility ( $n^{-1}$  slope). Figure 2 shows that no gains in electrical resistivity were made for carrier concentrations ranging from  $10^{19} \text{ cm}^{-3}$  up to  $10^{21} \text{ cm}^{-3}$ . In contrast, column III elements, Al, Ga and In, as well as Sn were successfully introduced to lower the electrical resistivity value down to  $3$  to  $5 \times 10^{-3} \Omega \cdot \text{cm}$ .

Using a simple substitutional defect scheme, one would expect Al, Ga, and In to result in p-type conductivity as they replace the Ge in  $\text{Ru}_2\text{Ge}_3$ . However, Ga- and Al-doped samples were often of n-type conductivity at room temperature. Similar results were also obtained in samples heavily doped with elements such as Rh, Co or even Sn. Because Hall effect measurements consistently showed high electrical resistivity ( $> 100 \times 10^{-3} \Omega \cdot \text{cm}$ ) and low mobility ( $< 1-2 \text{ cm}^2 \text{ V}^{-1} \text{ s}^{-1}$ ), these findings are attributed to one or several of the following mechanisms: a) excess dopant formed second phases (metallic compounds with Ru or Ge exist) of metallic behavior and very poor mobility; b) samples are compensated, resulting in very small Hall coefficient, high electrical resistivity and thus very low mobility; c) localized levels deep in the band gap have been created; d) n-type carrier mobility is very low. Additional experiments would be required to resolve these findings.

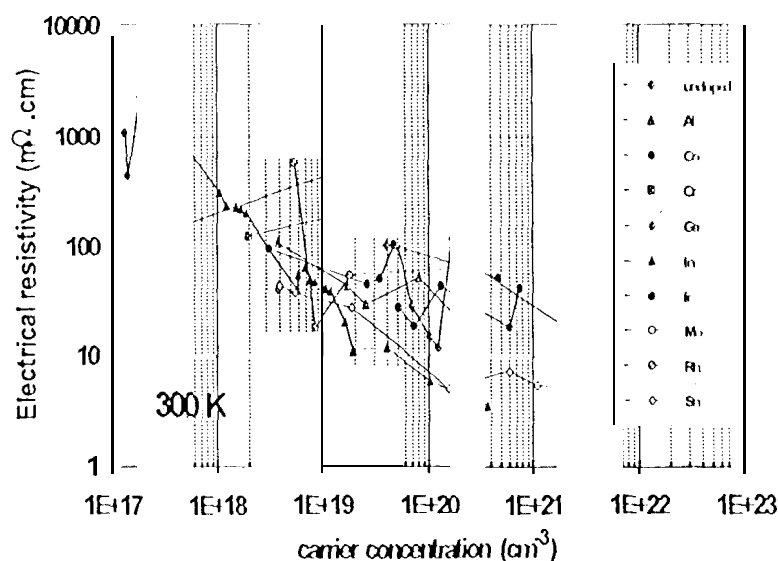


Figure 2 Room temperature electrical resistivity versus carrier concentration for doped and undoped  $\text{Ru}_2\text{Ge}_3$  samples.

The rationale for the use of Sn was that solid solutions exist between the isostructural  $\text{Ru}_2\text{Ge}_3$  and  $\text{Ru}_2\text{Sn}_3$  compounds (at least up to 8 mol.% of  $\text{Ru}_2\text{Sn}_3$ ). The  $\text{Ru}_2\text{Sn}_3$  compound is a very heavily doped semiconductor in its low temperature phase and has metallic behavior in its high temperature phase [7]. Sn additions into  $\text{Ru}_2\text{Ge}_3$  were likely to produce higher carrier concentrations in the "undoped" solid solution (as well as lower thermal conductivity). The lowest electrical resistivity values were obtained in p-type samples doped with nominal amounts of In and Sn in the 1 to 2 at.% range, however, even in these samples the best mobility values were about  $4$  to  $8 \text{ cm}^2\text{V}^{-1}\text{s}^{-1}$  for carrier concentrations in the  $10^{20} \text{ cm}^{-3}$  range.

#### High temperature Hall effect

Several good quality  $\text{Ru}_2\text{Ge}_3$  samples were measured from 100 K to 1000 K. Figure 3 presents electrical resistivity values as a function of the inverse of temperature and Figure 4 plots Hall mobility values as a function of temperature. At the highest temperatures, typical electrical resistivity and Hall mobility values of  $2.5 \times 10^{-3} \text{ } \Omega\cdot\text{cm}$  and  $10 \text{ cm}^2\text{V}^{-1}\text{s}^{-1}$  are obtained, regardless of doping levels. This is because the high temperature tetragonal phase has an intrinsic semiconducting behavior, even for the most heavily doped samples prepared in this effort. A bandgap value of  $0.58 \text{ eV}$  was derived. Below  $500 \text{ K}$ , the low temperature orthorhombic structural phase of  $\text{Ru}_2\text{Ge}_3$  shows that intrinsic behavior is reached for temperatures higher than  $400 \text{ K}$ .

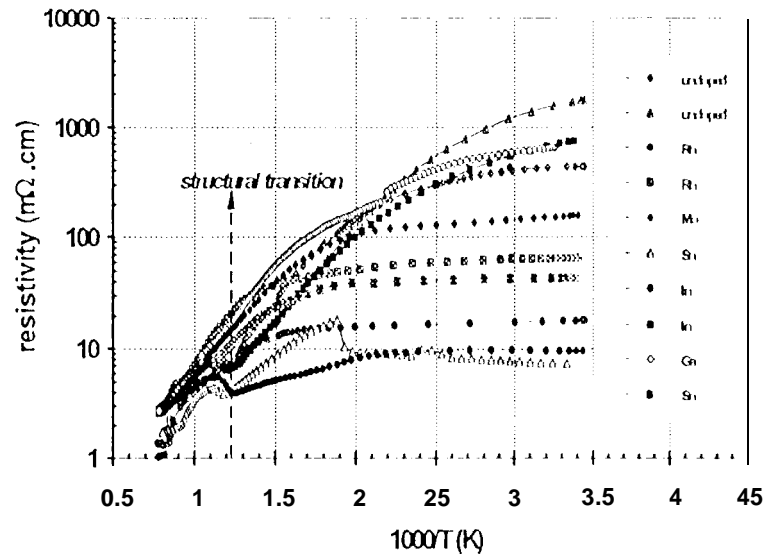


Figure 3 | High temperature electrical resistivity versus inverse of temperature for doped and undoped  $\text{Ru}_2\text{Ge}_3$  samples. Measurements were carried out either || or  $\perp$  to the  $[1\ 10]$  direction of crystal growth.

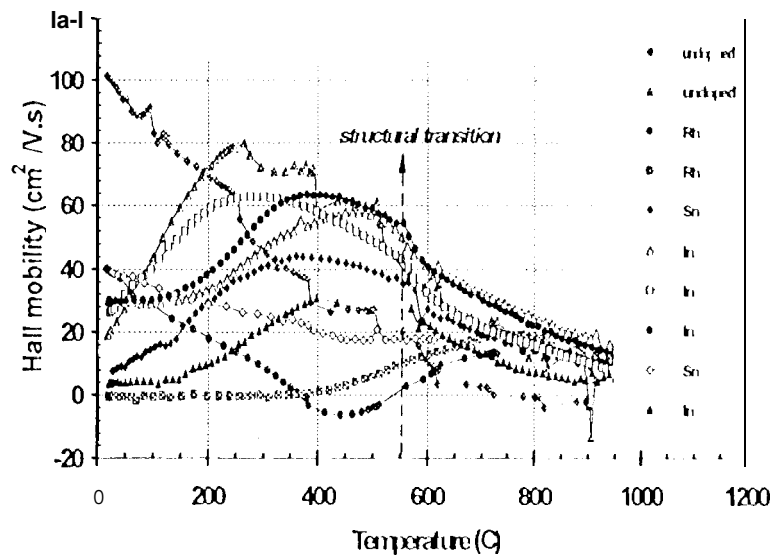


Figure 4 | High temperature Hall mobility versus temperature for doped and undoped  $\text{Ru}_2\text{Ge}_3$  samples. Measurements were carried out either || or  $\perp$  to the  $[1\ 10]$  direction of crystal growth.

A bandgap value of 0.71 eV was derived from the compared with a value of 0.89 eV determined by photochemical measurements conducted earlier [9]. Samples with the lowest electrical resistivity values did not show any true intrinsic

behavior-. Instead, the straight part of the curve on Figure 3 corresponds to the thermal ionization energy of the impurities used for doping  $\text{Ru}_2\text{Ge}_3$ . Similar results can be distinguished albeit with more difficulty on the other curves. Results are displayed in Table 1.

Table 1: Thermal ionization energies

Dopant	Ga	In	Rh
$\xi_a$ (eV)	0.14	0.08	0.05

The increase of Hall mobility with temperature for the low temperature phase indicate that the samples are compensated at room temperature. Because the bandgap is much too large to account for this at room temperature, these results appear to show that a more complex band structure exists such as deep localized levels, metallic in character, situated in the bandgap. When temperature increases, their contribution diminishes as carriers fill the higher mobility and lower effective mass main valence band. This indicates that the optimum thermoelectric properties of  $\text{Ru}_2\text{Ge}_3$  will be obtained for the low temperature phase when compensation effects are minimized, that is between 400 and 500 C.

#### Seebeck coefficient

It is quite remarkable how the variations of the Seebeck coefficient with temperature in Figure 5 are qualitatively similar to those of the Hall mobility in Figure 4. However, much larger values are obtained for the Seebeck coefficient than for the mobility for n-type samples. This can be interpreted as n-type material having large effective masses, thus quenching the mobility but enhancing the Seebeck coefficient. Thus, the beginning of the high temperature intrinsic regime due to compensation by p-type carriers of significantly lower effective masses would be much more rapid for the Hall mobility than for the Seebeck coefficient. At the lowest temperatures, most samples showed surprisingly low Seebeck values as well as low Hall mobility values. Nearly identical observations were made for  $\text{Ru}_2\text{Si}_3$  [2, 10]. Considering the large bandgap values of 0.72 eV and 1.08 eV of  $\text{Ru}_2\text{Ge}_3$  and  $\text{Ru}_2\text{Si}_3$ , respectively, it appeared difficult to reconcile semiconductor-like effects at low temperature and intrinsic conduction at high temperature. Preliminary theoretical attempts working only in terms of several valence and/or conduction bands were not able to reproduce this behavior. This could be explained, as noted before, by the existence of deep localized levels metallic in behavior. Additional data on more heavily doped samples would be required.

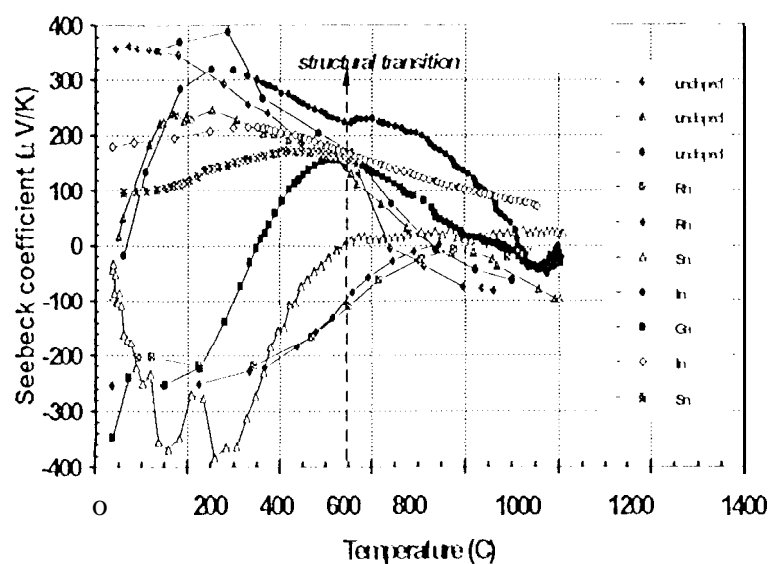


Figure 5: High temperature Seebeck coefficient versus temperature for doped and undoped  $\text{Ru}_2\text{Ge}_3$  samples (measured || to the [110] direction of crystal growth).

Still  $\text{Ru}_2\text{Ge}_3$  is an interesting thermoelectric material as a maximum absolute Seebeck values of  $400 \mu\text{V/K}$  can be achieved for both n-type and p-type samples. The low Seebeck values due to intrinsic conduction of the high temperature structural phase rule out any hope of achieving high figure of merit values. Best results for  $\text{Ru}_2\text{Ge}_3$  are to be expected between 200 and 500 °C.

#### Thermal conductivity

Thermal conductivity was measured on several samples with various doping levels. The experimental heat capacity value was very slightly larger than the high temperature Dulong-Petit value of  $0.297 \text{ Jg}^{-1}\text{K}^{-1}$ . Figure 6 clearly shows that most of the samples had similar thermal conductivity values. A minimum of about  $20 \times 10^{-3} \text{ W.cm}^{-1}\text{K}^{-1}$  at 400 °C is obtained for the low temperature orthorhombic phase. This is a low value but it was expected for the complexity of the  $\text{Ru}_2\text{Ge}_3$  unit cell and the weight of the Ru and Ge elements.



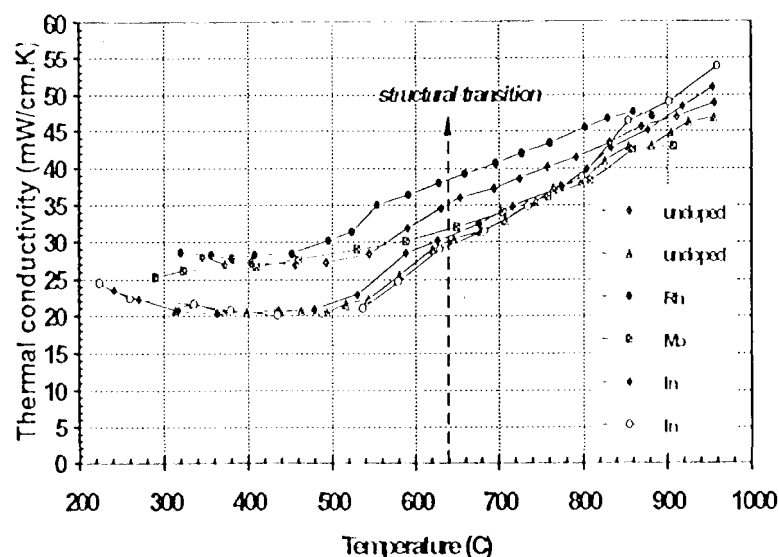


Figure 6 High Impedance thermal conductivity versus temperature for doped and undoped  $\text{Ru}_2\text{Ge}_3$  samples (measured  $\parallel$  to the  $[110]$  direction of crystal growth).

The electronic contribution (bipolar term due to intrinsic conduction) fully dominates the increase of the thermal conductivity with temperature for the high temperature tetragonal phase. Some of the ingots grown from melts slightly rich in Ge had inclusions of pure Ge. The presence of such inclusions consistently resulted in thermal conductivity 20% higher.

#### Anisotropic effects and figure of merit

Because of the elongated structure of the orthorhombic  $\text{Ru}_2\text{Ge}_3$  unit cell, anisotropic transport properties could be expected. Several ingots were cut so that samples could be measured in directions  $\parallel$  and  $\perp$  to the  $[110]$  direction of crystal growth. One of the samples (RUG18 labeled "7" in Table 2) was even cut at a  $45^\circ$  angle to the direction of crystal growth to evaluate the results of an average orientation.

Results are reported in Table 2 for room temperature Hall effect measurements. Differences in carrier concentration (or Hall coefficient) and electrical resistivity are no larger than 50%. For a equivalent carrier concentration, it appears that mobility values in the  $\parallel$  orientation are always slightly larger than those in the  $\perp$  orientation. However, much larger differences in carrier concentration, mobility and electrical resistivity were obtained for sample RUG16. This could be explained by the fact that RUG16 samples were large single crystalline plates while the other samples were composed of several grains. Some

disorientation Of these grains would result in average properties and thus less variations between the  $\perp$  and  $\parallel$  cuts.

Table 2: Anisotropy of the transport properties of p-type  $\text{Ru}_2\text{Ge}_3$

Sample 1/	orientation	n	$\mu_{11}$	P
RUG16 In-doped	$\perp$	$3.99 \times 10^{17}$	14.46	1083
	$\parallel$	$5.79 \times 10^{18}$	26.24	41.0
RUG17 In-doped	$\perp$	$6.91 \times 10^{18}$	14.00	64.6
	$\parallel$	$7.58 \times 10^{18}$	16.32	50.5
RUG18 In-doped	$\perp$	$1.05 \times 10^{18}$	19.08	310.3
	$\parallel$	$1.67 \times 10^{18}$	17.24	217.4
	/	$1.49 \times 10^{18}$	18.47	226.1
RUG121 Sn-doped	$\perp$	$3.97 \times 10^{18}$	35.26	44.5
	$\parallel$	$3.91 \times 10^{18}$	38.46	41.6

Because much larger differences were observed for RUG16 samples, all their high temperature thermoelectric properties were measured. Results are illustrated in Figures 7, 8, 9 and 10. The variations of carrier concentration as a function of the inverse of temperature are displayed on Figure 7. At the beginning of the measurement, the carrier concentration measured in the  $\parallel$  orientation is about 12 times larger than in the  $\perp$  orientation. However, this difference shrank rapidly as temperature increased (heating curves labeled “h”). At 350 C, values in the two orientations are much closer, within 10 to 20%. This small difference remained up to 1000 C and back to room temperature (cooling curves labeled “c”).

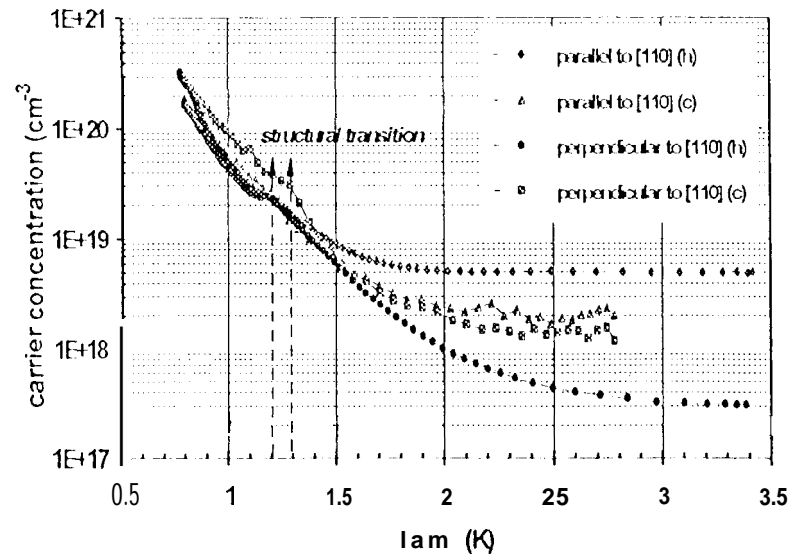


Figure 7 High temperature carrier concentration versus temperature for In-doped  $\text{Ru}_2\text{Ge}_3$  samples (RUG16). Measurements  $\parallel$  and  $\perp$  to the  $[110]$  direction of crystal growth are compared.

On Figure 8, Hall mobility values for both  $\parallel$  and  $\perp$  orientations are plotted as a function of temperature. Taking into account the simultaneous changes in carrier concentration on Figure 7, the Hall mobility measured in the  $\parallel$  orientation is about 50% higher than the mobility measured in the  $\perp$  orientation. This results in much lower values of the electrical resistivity in the  $\parallel$  orientation.

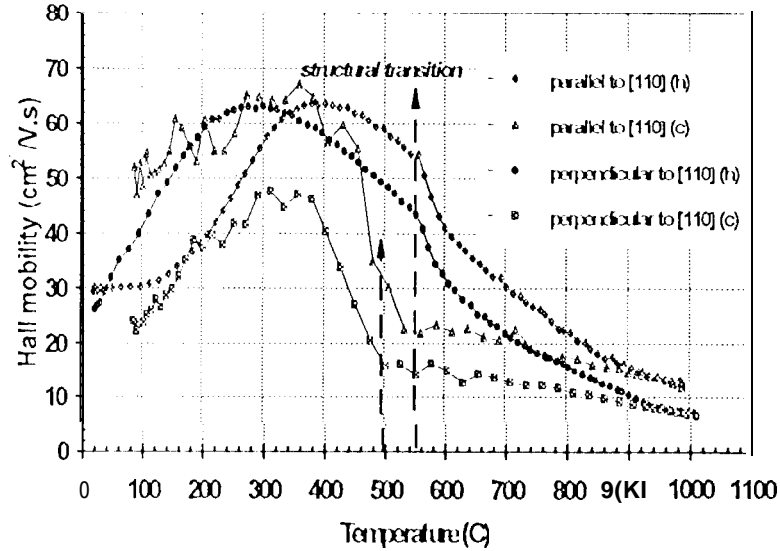


Figure 8 High temperature Hall mobility versus temperature for In-doped  $\text{Ru}_2\text{Ge}_3$  samples (RUG16). Measurements  $\parallel$  and  $\perp$  to the  $[110]$  direction of crystal growth are compared.

The variations of the Seebeck coefficient in temperature were found to follow closely those of the mobility (Figure 8), values measured in the  $\parallel$  orientation being about 200% higher than the mobility measured in the  $\perp$  orientation. No significant difference between the  $\parallel$  and  $\perp$  orientations was measured for the thermal conductivity. This was expected since the increase in electronic contribution to the total thermal conductivity due to lower electrical resistivity values in the  $\parallel$  orientation was still negligible compared to the lattice thermal conductivity.

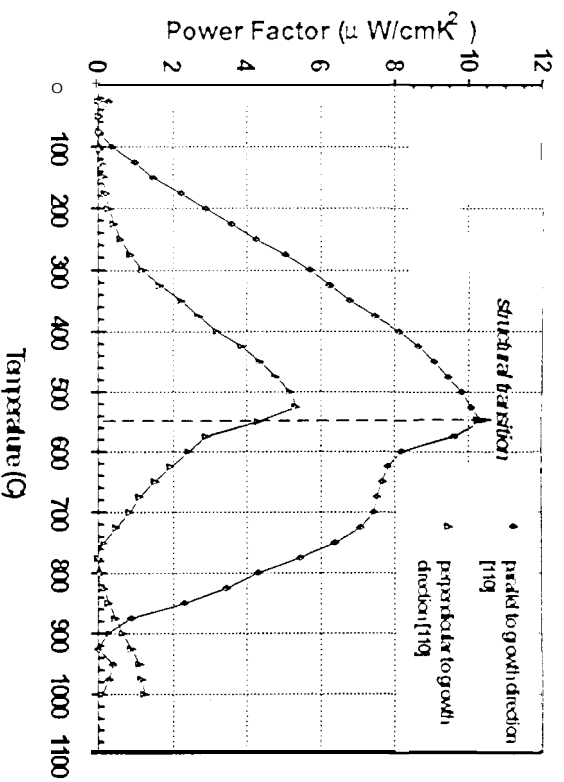


Figure 9 Calculated power factor values versus temperature for In-doped  $\text{Ru}_2\text{Ge}_3$  samples. Results for directions,  $\parallel$  and  $\perp$  to the  $[110]$  direction of crystal growth are plotted.

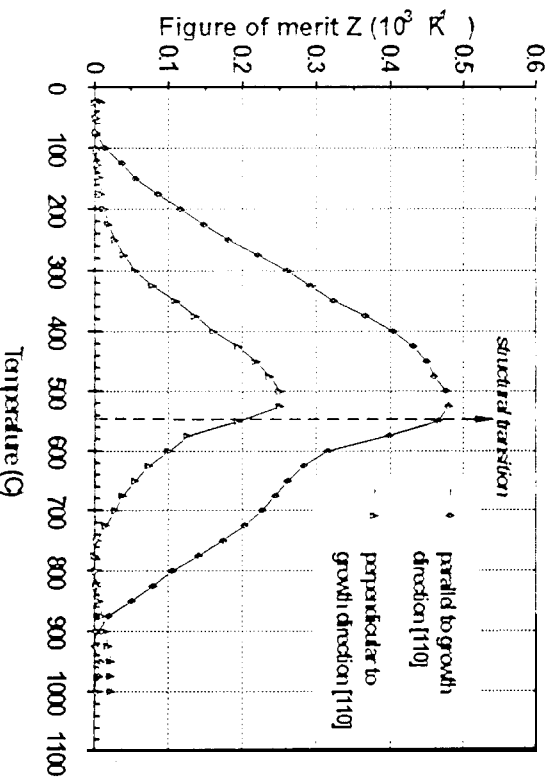


Figure 10 Calculated  $ZT$  values versus temperature for In-doped  $\text{Ru}_2\text{Ge}_3$  samples. Results for directions  $\parallel$  and  $\perp$  to the  $[110]$  direction of crystal growth are plotted.

Some hysteresis was also observed for the structural phase transition. Although its effect on the transport properties was simultaneous in temperature for both the  $\parallel$  and  $\perp$  orientations, it occurred at a temperature close to 550 °C upon heating of the

samples and at a temperature slightly below **500 C** upon cooling of the samples (see Figures 7 and 8).

As a consequence of these findings, the best power factor and figure of merit values were obtained||to the preferential direction of crystal growth, as seen on Figures 9 and 10 respectively. A maximum ZT value of about 0.4 was obtained at 500 C along the [1 10] orientation.

### CONCLUSION

The work on  $\text{Ru}_2\text{Ge}_3$  showed that single crystals of this material could be prepared using unseeded directional crystallization from slightly off-stoichiometric Ge-rich melts. An extensive X-ray analysis determined the preferential direction of crystal growth as [110]. High temperature measurements of the transport properties of doped and undoped  $\text{Ru}_2\text{Ge}_3$  samples determined that both the high temperature tetragonal phase and the low temperature orthorhombic phase were p-type semiconductors. Bandgap values of about 0.59 eV and 0.71 eV were calculated from Hall effect and electrical resistivity measurements. However, it was found that only the orthorhombic structural phase of  $\text{Ru}_2\text{Ge}_3$  had a good potential for thermoelectric applications with large Seebeck coefficient (both p-type and n-type) and low thermal conductivity. Unfortunately, the low values of the carrier mobility, the inability to achieve optimum doping levels and the rapid decrease of the mobility with increasing carrier concentration maintained a high electrical resistivity and limited the dimensionless figure of merit to a maximum "experimental" value of 0.4 at 500 C.

### ACKNOWLEDGMENTS

The work described in this paper was carried out by the Jet Propulsion Laboratory/ California Institute of Technology, under a contract with the National Aeronautics and Space Administration. This effort was sponsored by the Knolls Atomic Power Laboratory, Schenectady, New York. The authors would like to thank Jim Kullick for crystallographic analyses, Denise Irvine, Danny Zoltan and Andy Zoltan for preparation and measurement of the samples.

### REFERENCES

- [1] C.B. Vining and J.P. Fleurial, "Silicon-Germanium: an Overview of Recent Developments", *10<sup>th</sup> Symposium on Space Nuclear Power Systems, Special Volume*, Albuquerque, New Mexico, January 10-14 (1993).

- [2] C.B. Vining and C.E. Allevato, "Intrinsic Thermoelectric Properties of Single Crystal  $\text{Ru}_2\text{Si}_3$ ", *Proceedings of the X<sup>th</sup> International Conference on Thermoelectrics*, Cardiff, Wales, UK, September 10-12, 167-173 (1991).
- [3] P. Caillat, A. Borshchevsky and J.-P. Fleurial, "Search for New High Temperature Thermoelectric Materials", *Proceedings of the 271<sup>st</sup> Intersociety Energy Conversion Engineering Conference*, San Diego, California, August 3-7, (3) 499-503 (1992),
- [4] C.B. Vining, "Silicides as Promising Thermoelectric Materials", *Proceedings of the IX<sup>th</sup> International conference on Thermoelectrics*, Pasadena, California, March 19-21, (1), 249-259 (1990).
- [5] D.J. Poutcharovsky and E. Parthe, "The Orthorhombic Crystal Structure of  $\text{Ru}_2\text{Si}_3$ ,  $\text{Os}_2\text{Si}_3$  and  $\text{Os}_2\text{Ge}_3$ ", *Acta Cryst.*, 1130, 2692 (1974).
- [6] D.J. Poutcharovsky, K. Yvon and E. Parthe, "Diffusionless Phase Transformations of  $\text{Ru}_2\text{Si}_3$ ,  $\text{Ru}_2\text{Ge}_3$  and  $\text{Ru}_2\text{Sn}_3$ . I. Crystal Structure Investigations", *J. Less Common Metals*, 40, 139 (19/5).
- [7] C.J. Susz, J. Muller, K. Yvon and E. Parthe, "Diffusionless Phase Transformations of  $\text{Ru}_2\text{Si}_3$ ,  $\text{Ru}_2\text{Ge}_3$  and  $\text{Ru}_2\text{Sn}_3$ . II. Electrical and Magnetic Properties", *J. Less Common Metals*, 71, P1 (1980).
- [8] *Binary Alloy Phase Diagrams*, 2nd edition, Ed. T.B. Massalski, ASM Int., p. 1992 (1990).
- [9] A. Borshchevsky and J.-P. Fleurial, " $\text{Ru}_2\text{Ge}_3$ : Crystal Growth and Sonic Properties" accepted for publication in *Journal of Crystal Growth* (1993).
- [10] C.B. Vining, "Extrapolated thermoelectric figure of Merit of Ruthenium Silicide" *Proceedings of the 9<sup>th</sup> Symposium on Space Nuclear Power Systems*, Albuquerque, New Mexico, January 12-16, (1), 338-342 (1991).